CENTRAL ASIAN TRANSACTIONS ON MATERIALS STRUCTURE AND PROPERTIES

https://doi.org/10.51885/3134-7983_CATMSP_2026_1_6
SRSTI 53.31.23

SELECTIVE REDUCTION OF IRON FROM IRON–MANGANESE ORE USING HYDROGEN

Yerbol Kuatbay [1], **Asylbek Nurumgaliev** [2], **Gulzat Bulekova** [1]*, **Ainagul Otarbayeva** [3], **Semyon Salikhov** [4]

[1]Karaganda Industrial University, Temirtau, Kazakhstan
[2]Abilkas Saginov Karaganda Technical University, Karaganda, Kazakhstan
[3]K. Zhubanov Aktobe Regional University, Aktobe, Kazakhstan
[4]South Ural State University (National Research University), Chelyabinsk, Russian Federation
*Corresponding author: Gulzat Bulekova, e-mail: g.bulekova@tttu.edu.kz

Keywords:
iron–manganese ore, hydrogen, manganese, iron, arsenic, phosphorus, reduction.

ABSTRACT

The results of the study indicate that the iron–manganese ore is characterized by a complex mineralogical composition comprising Fe-, Mn-, and Si-bearing oxides as well as complex aluminosilicate phases. X-ray diffraction (XRD) of the as-received material confirmed goethite (FeO(OH)), hematite (Fe_2O_3), quartzite (SiO_2), and manganese dioxide (MnO_2) as the dominant phases.

During oxidative roasting, goethite underwent dehydroxylation with the formation of hematite, and the emergence of Mn_2O_3 and Mn_3O_4 phases was also identified. The formation of Mn_7SiO_{12} indicates high-temperature interaction between manganese species and silica, suggesting the development of solid-state synthesis processes in the Mn–Si–O system.

Thus, hydrogen proved to be an efficient and environmentally benign reductant, enabling selective iron reduction at relatively low temperatures. The reduced metal and the oxide residue can be separated by smelting or magnetic separation, which opens prospects for developing processing flowsheets for Kazakhstan's iron–manganese ores with minimal environmental impact.

INTRODUCTION

Hydrogen is currently considered one of the key instruments enabling low-carbon transformation of the global energy system. According to projections by the International Renewable Energy Agency (IRENA), by 2050 the share of hydrogen in global energy consumption could increase to 12% (IRENA, 2023). The European Union countries and other advanced industrial economies are actively investing in technological solutions in this field, which strengthens the prospects for the widespread use of hydrogen as an energy carrier. In October 2024, Kazakhstan also adopted a national Concept for the Development of Hydrogen Energy to accelerate the transition to a low-carbon economy, initiating targeted measures at the national level. In this concept, hydrogen is defined as a strategic element for decarbonizing industry and the transport sector (Baisanov et al., 2021).

One of the major initiatives in Kazakhstan is the world's largest green hydrogen production hub in Mangystau Region, implemented by Svevind Group. The project includes a seawater desalination plant with a capacity of 255,000 m^3 per day, wind and solar power plants with a total installed capacity of 40 GW, and 20 GW of electrolyzer systems. In addition, KazMunayGas Engineering is considering underground water as an alternative source for hydrogen production under water scarcity conditions (KMG Engineering, 2024). These initiatives demonstrate the growing strategic role of hydrogen in Kazakhstan's energy system.

In the metallurgical sector, the use of hydrogen as a reducing agent has been actively studied in recent years. In the processing of iron and manganese ores, hydrogen exhibits the ability to selectively reduce iron (Ngoy et al., 2020; Ernst et al., 2024). It has been shown that in complex minerals containing hematite, magnetite, and titanium-bearing phases, hydrogen demonstrates higher kinetic efficiency compared to traditional carbon-based reductants (Naseri Seftejani & Schenk, 2018; John & Hayes, 1982). While carbon-based reduction releases CO_2 as a by-product, hydrogen reduction produces water, which not only enhances the environmental advantages of the technology but also significantly reduces greenhouse gas emissions from metallurgical processes (Matthew et al., 1990). Furthermore, hydrogen's ability to selectively separate iron from manganese enables better control of phase composition and reduces energy consumption.

The mineralogical structure of iron–manganese ores in Kazakhstan is complex and characterized by high concentrations of iron and silicon, which makes traditional blast furnace or electric furnace processing inefficient (Yerbolat et al., 2024; Pavlov et al., 2012). Such methods lead to increased energy consumption, higher manganese losses, and additional environmental pollution (Suleimen & Salikhov, 2022; Kosdauletov et al., 2021). Although physical and physicochemical beneficiation methods can partially separate mineral phases based on density or magnetic properties, the heterogeneous structure of the ore limits their effectiveness (Baisanov et al., 2021; Tastanova et al., 2023).

Carbon-based reduction also has well-known drawbacks, including high CO_2 emissions and incomplete recovery of manganese, which negatively affect metallurgical performance (Kosdauletov & Roshchin, 2020; Kosdauletov et al., 2022). Previously proposed two-stage pyrometallurgical schemes—initial reduction of iron and phosphorus followed by melting of the product—have environmental and technological limitations, since the use of CO as a reductant causes persistent environmental harm (Roshchin et al., 2023). In this context, the transition to hydrogen is considered a more environmentally friendly and efficient approach to processing iron–manganese ores.

MATERIALS AND METHODS

For the experiments, iron–manganese ore from the "Keregetas" deposit in Kazakhstan was used. Prior to testing, the ore was ground in an IDA-175 mill to a particle size of −1 mm to ensure homogeneity of its chemical composition. The ground material was then moistened, placed in a mold, and dried at 150 °C for 1 hour to completely remove moisture.

The reduction process was carried out in an RB Automazione MM 6000 laboratory vertical furnace designed for testing iron-bearing materials (Figure 1). Samples weighing up to 30 g were placed in a reaction tube made of heat-resistant AISI 310 steel with a diameter of 75 mm. The temperature was controlled by a system consisting of five independent heating zones equipped with silicon carbide heaters, ensuring uniformity of the thermal field.

Reduction was performed in the temperature range of 700–1100 °C with a holding time of 60 minutes. High-purity hydrogen (99.99%), compliant with GOST 3022-80, was used as the reducing agent. It was supplied at a flow rate of 0.5 L/min and monitored using a digital mass flow controller. High-grade argon (99.993%), compliant with GOST 10157-2016, was used as the inert gas.

The furnace was equipped with an automated control system that allowed programming of the temperature profile, real-time monitoring of process parameters, and continuous recording of sample mass changes during the experiment.

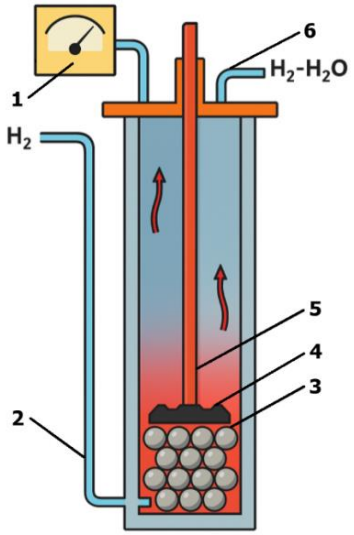

Figure 1. Schematic diagram of the reactor setup for the experiment: 1 – multimeter; 2 – hydrogen gas supply system; 3 – corundum balls for uniform gas distribution; 4 – samples; 5 – thermocouple; 6 – exhaust system for outlet (residual) gases
Note – prepared by the authors

The microstructure and elemental composition were investigated using a JEOL JSM-7001F scanning electron microscope equipped with an OXFORD X-Max 80 energy-dispersive detector. The analysis was performed at an accelerating voltage of 30 kV with magnification up to 1.2 nm. Composition was determined in both point and area analysis modes, and data processing was carried out using the microscope's proprietary software.

X-ray diffraction analysis (XRD) was conducted on a Rigaku Ultima IV diffractometer with a CuKα X-ray tube (λ = 1.5406 Å). Measurements were performed at 40 kV and 30 mA. Diffractograms were recorded over the range 2θ = 5–90° at a scanning rate of 5°/min. Powder samples (< 0.063 mm fraction) were placed in flat sample holders for analysis. Phase identification was carried out using the Match software (Crystal Impact, Germany) with the PDF2 (2009) database, which enabled the detection of newly formed oxide and silicate phases resulting from the reduction process.

Ores from the "Keregetas" deposit are characterized by a complex mineralogical composition and heterogeneous structure. They contain iron, manganese, silicon, barium, potassium, and aluminum. The presence of phosphorus and arsenic impurities complicates their metallurgical processing.

To obtain an averaged chemical composition, the raw ore was melted in a Nabertherm resistance furnace at 1650 °C in a corundum crucible. The melt was then rapidly cooled in a metal mold. The resulting quenched material was analyzed using a JEOL JSM-7001F scanning electron microscope equipped with an OXFORD X-Max 80 energy-dispersive detector. The study was conducted at accelerating voltages of 0.5–30 kV over a sample area magnified up to 600 μm, enabling high-precision determination of the elemental composition.

The average chemical composition of the ore after melting and quenching is presented in Table 1.

Table 1. Elemental composition of the ore

Analysis of the sample area	O	Al	Si	K	Ca	Mn	Fe	As	Ba
at.% (atomic percent)	66,6	4,5	9,9	0,9	0,5	11,8	5,4	0,4	0,1
wt.% (weight percent)	42,5	4,8	11,1	1,5	0,7	25,8	12,0	1,1	0,5
Note – prepared by the authors									

Figure 2 presents the results of X-ray diffraction (XRD) analysis of the initial iron–manganese ore. The analysis was performed using a Rigaku Ultima IV diffractometer with Match software. Based on the results, the main mineral phases of the ore were identified as goethite FeO(OH), hematite Fe_2O_3, manganese dioxide MnO_2, a combined iron–manganese oxide phase $FeMnO_3$, and silicon dioxide SiO_2.

Due to the relatively low peak intensities of other compounds, accurate identification of phases containing potassium (K), aluminum (Al), arsenic (As), and barium (Ba) was difficult.

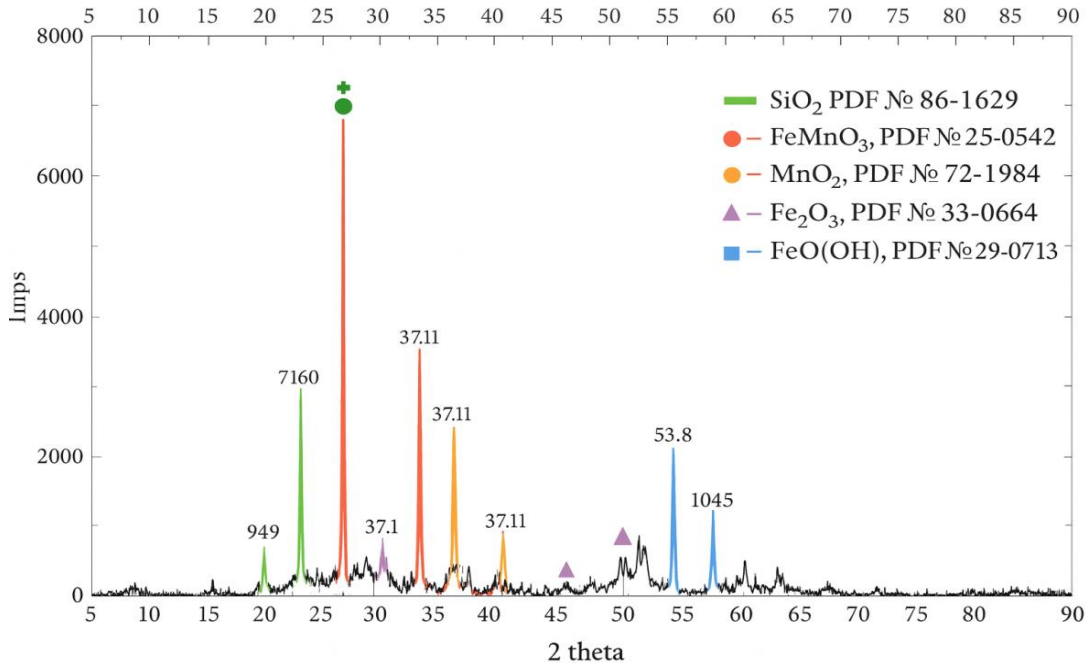

Figure 2. X-ray diffraction pattern of the initial iron–manganese ore
Note – prepared by the authors

To investigate the changes occurring in iron–manganese ores during heating in an air atmosphere, homogeneous lump samples from the "Keregetas" deposit were placed in a corundum crucible and heated in a Nabertherm muffle furnace. The heating rate was 200 °C/h, the target temperature was 1000 °C, and the holding time at this temperature was 2 hours.

RESULTS AND DISCUSSION

According to the X-ray diffraction data (Figure 3), the following phases were identified in the samples after calcination in an air atmosphere: Fe_2O_3, Mn_2O_3, Mn_3O_4, $FeMnO_3$, and Mn_7SiO_{12}.

During oxidative heating, oxygen is released from the crystal lattice of manganese dioxide (MnO_2), resulting in its partial reduction to lower oxides (Mn_3O_4 and Mn_2O_3). In addition, goethite FeO(OH) loses structural water and transforms into hematite (Fe_2O_3).

As a result of calcination in an air atmosphere, the total mass loss amounted to 13.24%, which is associated with dehydration and partial reduction of manganese oxides.

X-ray diffraction analysis, elemental distribution maps, and microstructural studies of the initial iron–manganese ore from the "Keregetas" deposit (Figures 1, 2, and 3) confirm its complex mineralogical composition and the predominance of iron and manganese in oxide forms. Such an ore structure can create certain technological difficulties in the production of manganese alloys from this raw material.

Therefore, experiments on the selective reduction of iron using hydrogen as a reducing agent were carried out. Reductive roasting was performed at temperatures of 700, 800, 900, 1000, and 1100 °C with a holding time of 60 minutes.

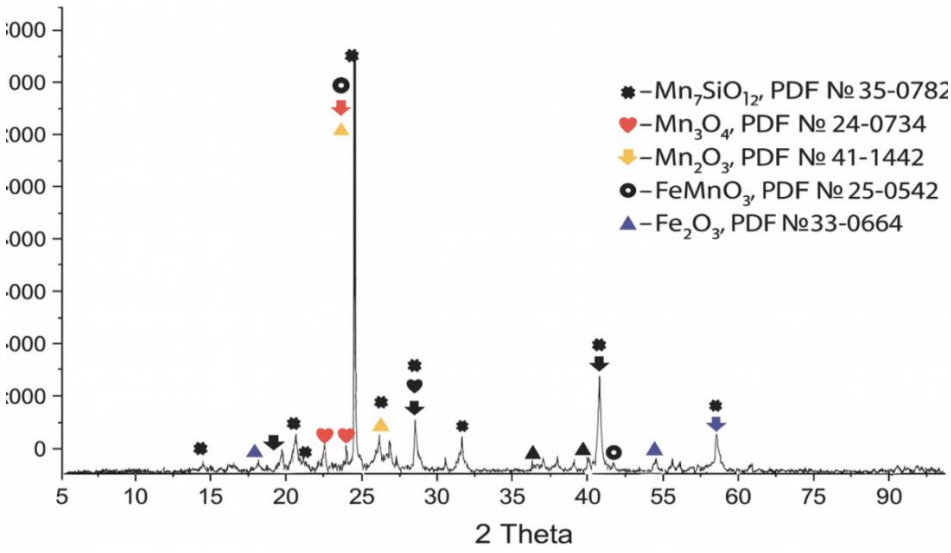

Figure 3. X-ray diffraction pattern of iron–manganese ore after oxidative calcination
Note – prepared by the authors

Figure 4 shows the dependence of sample mass loss on reduction temperature. At 700 °C, the mass loss was 18.41%, while increasing the temperature to 1000 °C led to a mass loss of 22.1%, which is associated with active reduction of iron and release of oxygen from oxides. However, when the temperature was further increased to 1100 °C, sintering of ore particles was observed, which reduced the interaction between hydrogen and the particle surfaces and hindered metal reduction, resulting in a decrease in mass loss to 19.8%.

Figure 4 presents the results of reductive roasting of iron–manganese ore samples from the "Keregetas" deposit in a hydrogen atmosphere at 700–1000 °C for 60 minutes at a hydrogen flow rate of 0.5 L/min.

Thermodynamic background (Fe–O–H and Mn–O–H systems)

The direction of metal reduction processes in a hydrogen atmosphere primarily depends on the equilibrium in metal–oxygen systems and the H_2/H_2O ratio in the gas phase. In general, the reduction of iron oxides by hydrogen proceeds through the following stages:

$$Fe_2O_3 \rightarrow Fe_3O_4 \rightarrow FeO \rightarrow Fe,$$

with the formation of water vapor (H_2O) as a reaction product. In the temperature range of 700–1000 °C, hydrogen effectively binds oxygen from iron oxides, enabling deep and intensive reduction to metallic iron. This is consistent with the increase in mass loss shown in Figure 4 and the formation of metallic Fe phase confirmed by XRD analysis (Figure 6).

For manganese oxides, reduction is thermodynamically more complex. Although MnO_2 and Mn_2O_3 can be relatively easily reduced to lower oxides (Mn_3O_4 and MnO), further reduction of MnO to metallic manganese requires a higher reducing potential in the gas phase (higher H_2/H_2O ratio) and higher temperatures. Therefore, at 700–800 °C, manganese remains

predominantly in oxide phases, whereas at temperatures above 900 °C, metallic manganese begins to appear (Table 2). This confirms the mechanism of selective reduction: iron is reduced first, followed by partial reduction of manganese at higher temperatures.

At 1100 °C, sintering of ore particles reduces gas–solid contact and increases diffusion resistance, which can slow down the reduction rate. In addition, at high temperatures, the formation of difficult-to-reduce complex silicate phases in the Fe–Mn–Si–O system (such as $FeMnSiO_4$ and Mn_2SiO_4) becomes more likely, which limits further metal reduction and may explain the observed decrease in mass loss at 1100 °C.

The general trend is consistent for all temperature regimes: as temperature increases, reduction processes in the ore become more intensive and deeper. After reduction, the formation of a metallic phase is observed both on the surface and inside the samples, with iron and arsenic being the main metallic components.

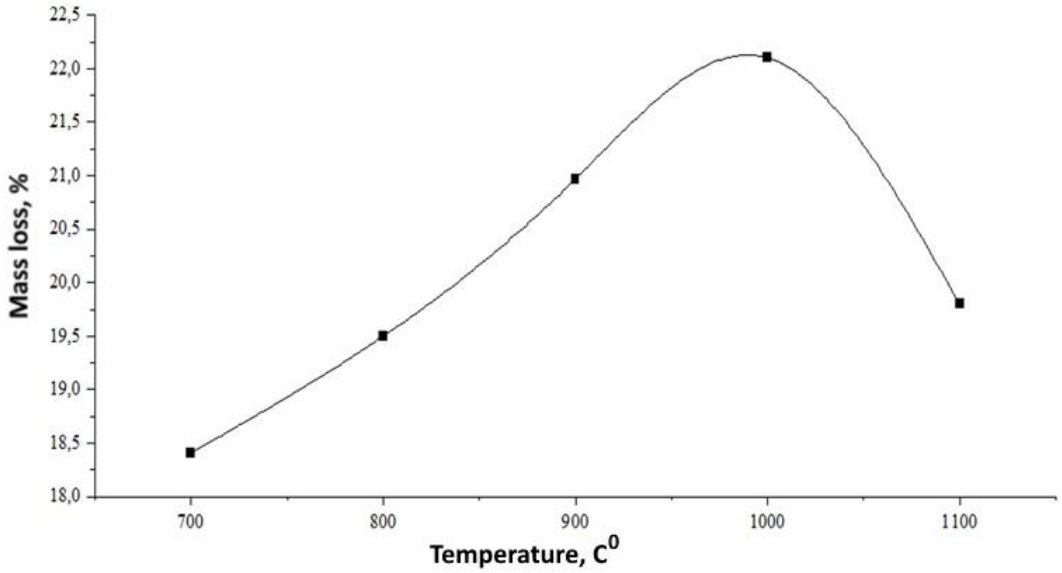

Figure 4. Mass loss of samples after reductive roasting in a hydrogen atmosphere (hydrogen flow rate 0.5 L/min)

Note – prepared by the authors

As the reduction temperature increases, a small amount of manganese appears in the metallic phase, indicating that its reduction begins at temperatures above 900 °C (Figure 5, Table 2).

In the micrographs shown in Figure 5, two main structural regions are observed: (i) light-colored metallic inclusions and (ii) a dark-colored oxide–silicate matrix. According to the micro-X-ray spectral analysis results presented in Table 2, at temperatures of 700–800 °C the metallic inclusions consist mainly of Fe (98.7–99.5 at.%) and As (0.5–1.3 at.%), indicating that hydrogen selectively reduces iron to the metallic state in this temperature range and promotes the accumulation of arsenic in the metallic phase.

In contrast, the dark matrix region exhibits high contents of O and Mn (approximately O ≈ 38–42 at.% and Mn ≈ 52–58 at.%), while the Fe content remains low. This suggests that the matrix is predominantly composed of manganese oxides and silicate phases, and that manganese largely remains in the oxide form at these temperatures.

At 900–1000 °C, the appearance of 2.8–4.4 at.% Mn in the metallic inclusions indicates the onset of partial reduction of manganese. Thus, the experimental results confirm that iron is predominantly reduced in the range of 700–900 °C, whereas manganese reduction becomes significant only at higher temperatures, demonstrating the selective nature of the process.

After roasting, the remaining oxide phase, regardless of temperature, mainly consists of manganese oxides and gangue silicate minerals, indicating that the ore material was partially, but not completely, reduced.

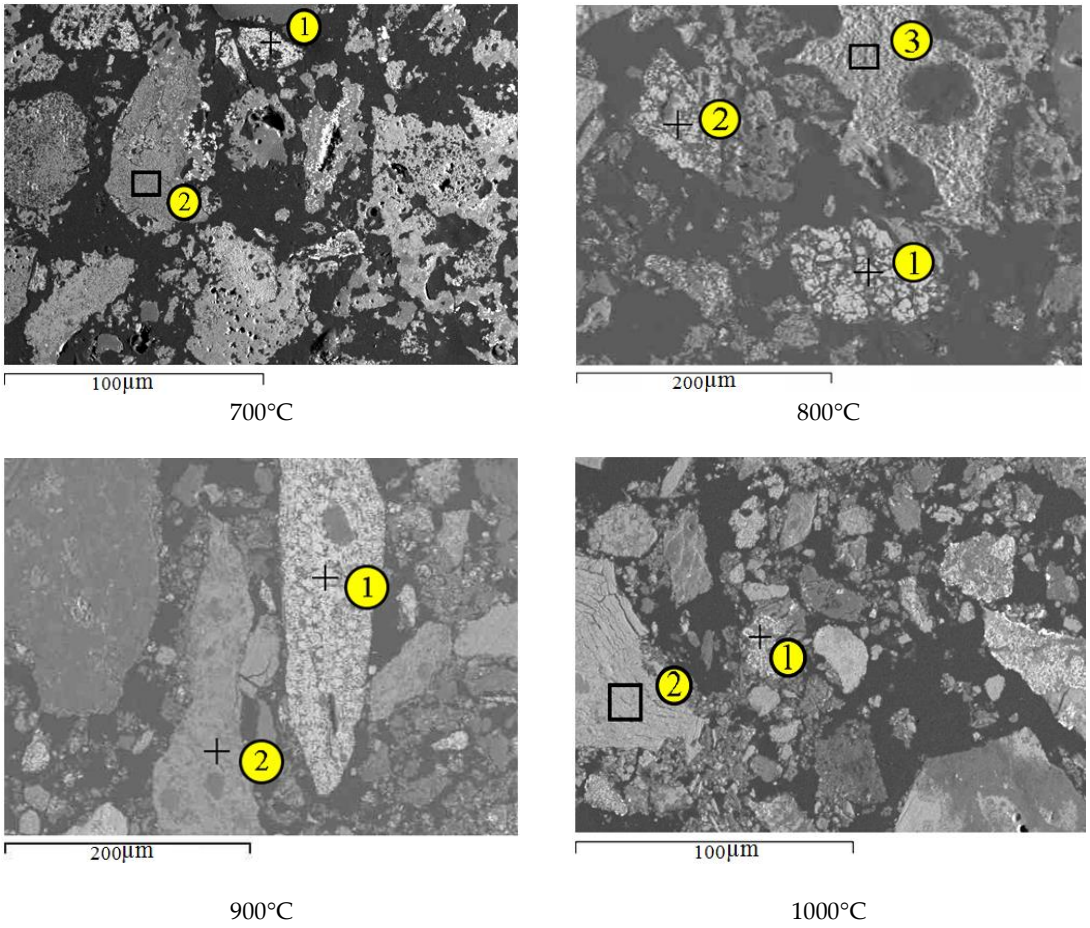

Figure 5. Microstructural appearance of phases in iron–manganese ore after reductive roasting

Note – prepared by the authors

Table 2. Results of micro-X-ray spectral analysis of the samples (Figure 5)

Sample	Element content, at.%						
	Analysis point	O	Al	Si	Mn	Fe	As
700°C	1	0,0	0,0	0,0	0,0	98,7	1,3
	2	39,5	0,0	2,4	52,1	6,1	0,0
800°C	1	0,0	0,0	0,0	0,0	99,5	0,5
	2	0,0	0,0	0,0	0,0	98,9	1,1
	3	42,0	2,0	0,7	53,0	2,2	0,0
900°C	1	0,0	0,0	0,0	2,8	95,3	1,9
	2	38,5	0,0	1,3	57,9	2,4	0,0
1000°C	1	0,0	0,0	0,0	4,4	93,6	2,0
	2	39,8	0,0	1,9	55,6	2,7	0,0
Note – prepared by the authors							

Figure 6 shows the diffractograms of iron–manganese ore samples after reductive roasting in a hydrogen atmosphere at temperatures of 700, 800, 900, 1000, and 1100 °C with a holding time of 60 minutes.

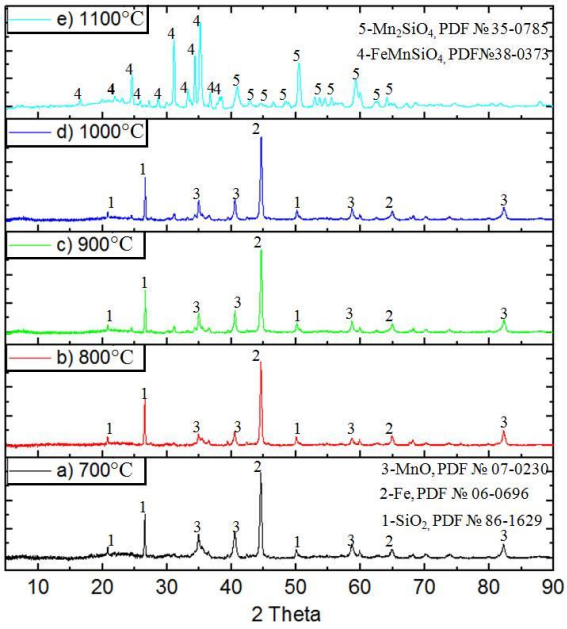

Figure 6. Diffractograms of samples after reductive roasting in a hydrogen atmosphere with a holding time of 60 minutes. Phases: 1 – SiO_2, 2 – Fe, 3 – MnO, 4 – $FeMnSiO_4$, 5 – Mn_2SiO_4.
Note – prepared by the authors

According to the X-ray diffraction data, reduction in a hydrogen atmosphere leads to the formation of metallic iron (Fe), manganese oxide (MnO), and quartz (SiO_2) phases in the samples. This indicates effective reduction of iron and partial reduction of manganese oxides at temperatures up to 1000 °C.

When the temperature is further increased to 1100 °C with the same holding time of 60 minutes, new complex phases such as $FeMnSiO_4$ and Mn_2SiO_4 appear in the ore.

Thus, it can be concluded that at 1100 °C the reduced components of iron, manganese, and silicon begin to interact, leading to the formation of difficult-to-reduce silicate compounds, which reduces the further efficiency of metal reduction.

CONCLUSIONS

Micro-X-ray spectral analysis of the iron–manganese ore from the “Keregetas” deposit revealed the presence of major elements such as Fe, Mn, Al, Si, Ba, and O. According to X-ray diffraction data, the initial ore contains the following phases: goethite (FeO(OH)), hematite (Fe_2O_3), manganese dioxide (MnO_2), a combined iron–manganese oxide phase ($FeMnO_3$), and silicon dioxide (SiO_2).

During oxidative calcination in an air atmosphere, dissociation of oxygen occurs from the crystal lattice of MnO_2, which reduces the oxidation state of manganese and leads to the formation of lower oxides such as Mn_3O_4 and Mn_2O_3. At the same time, goethite (FeO(OH)) undergoes dehydration and transforms into hematite (Fe_2O_3).

Reductive roasting of the ore in a hydrogen atmosphere at 700–900 °C with a holding time of 60 minutes makes it possible to obtain a soft oxide concentrate enriched in iron and manganese, which can subsequently be effectively separated by smelting or magnetic separation.

However, increasing the temperature to 1000 °C leads to partial reduction of manganese and its loss of up to 4.4 at.%, while further heating to 1100 °C causes sintering of ore particles, which worsens metal reduction and decreases overall mass loss.

Thus, the conducted experiments demonstrate that replacing carbon-containing reducing agents (C, CO) with hydrogen provides the following advantages:

- significant reduction of carbon dioxide emissions;
- improved environmental safety of metallurgical processes;
- selective reduction of iron without substantial loss of manganese;
- creation of prerequisites for developing low-carbon technologies for processing iron–manganese ores.

The development of hydrogen technologies and the decreasing cost of electricity from renewable sources open real opportunities for an economically viable transition to hydrogen use in Kazakhstan's metallurgy and for producing environmentally friendly ferroalloy concentrates.

CONFLICT OF INTEREST: The authors declare that they have no conflicts of interest.

FUNDING: This study was carried out within the framework of a grant-funded research project of the Ministry of Science and Higher Education entitled "Investigation of the possibility of obtaining high-manganese slags from non-conforming iron–manganese ores of Kazakhstan through selective reduction of iron using hydrogen gas" (project No. AR23490490).

ACKNOWLEDGMENTS: The authors sincerely thank Karaganda Industrial University, K. Zhubanov Aktobe Regional University, and South Ural State University (Laboratory of Hydrogen Technologies in Metallurgy) for their administrative and technical support, as well as for providing the necessary infrastructure and resources for this research.

DECLARATION ON THE USE OF ARTIFICIAL INTELLIGENCE TECHNOLOGIES: The authors did not use artificial intelligence (AI) tools at any stage of preparing this work.

REFERENCES

Baisanov, A., Maishina, Z., Isagulov, A., Smagulova, N., & Yudakova, V. (2021). Experimental melting of high-silicon ferromanganese with the use of ferromanganesian ore and manganese slag. Metalurgija, 60, 89–92.

Ernst, M.S., Tangstad, M., & Du Preez, S.P. (2024). Pre-reduction of Nchwaning manganese ore in CO/CO_2, H_2/H_2O, and H_2 atmospheres. Minerals Engineering, 216, 108854.

IRENA. (2023). World Energy Transitions Outlook 2023. International Renewable Energy Agency.

John, D. H. S., & Hayes, P.C. (1982). Microstructural features produced by the reduction of wustite in H_2/H_2O gas mixtures. Metallurgical Transactions B, 13, 117–124.

Kosdauletov, N. Y., & Roshchin, V. E. (2020). Estimation of selective reduction of iron and phosphorus from manganese ores of different genesis. IOP Conference Series: Materials Science and Engineering, 966(1), 012036.

Kosdauletov, N., Mukambetgaliyev, E.K., & Roshchin, V.E. (2021). Separation of ferromanganese ore components by non-contact and contact carbothermic reduction. Izvestiya. Ferrous Metallurgy, 64(10), 761–767.

Kosdauletov, N., Mukambetgaliyev, E.K., & Roshchin, V.E. (2022). Separation of ferromanganese ore components by reduction with carbon and carbon monoxide. Steel in Translation, 52(4), 416–421.

Matthew, S.P., Cho, T.R., & Hayes, P.C. (1990). Mechanisms of porous iron growth on wustite and magnetite during gaseous reduction. Metallurgical Transactions B, 21, 733–741.

Matthew, S.P., & Hayes, P.C. (1990). Microstructural changes occurring during the gaseous reduction of magnetite. Metallurgical Transactions B, 21, 153–172.

Naseri Seftejani, M., & Schenk, J. (2018). Thermodynamic of liquid iron ore reduction by hydrogen thermal plasma. Metals, 8(12), 1051.

Ngoy, D., Sukhomlinov, D., & Tangstad, M. (2020). Pre-reduction behaviour of manganese ores in H_2 and CO containing gases. ISIJ International, 60(11), 2325–2331. https://doi.org/10.2355/isijinternational.ISIJINT-2020-120

Sarkar, A., Schanche, T. L., & Safarian, J. (2023). Isothermal pre-reduction behavior of Nchwaning manganese ore in H_2 atmosphere. Materials Proceedings, 15, 58. https://doi.org/10.3390/materproc2023015058

Schanche, T. L., & Tangstad, M. (2021). Prereduction of Nchwaning ore in $CO/CO_2/H_2$ gas mixtures. Minerals, 11, 1097. https://doi.org/10.3390/min11101097

Suleimen, B., & Salikhov, S. P. (2022). Behavior of extrusion briquettes (Brex) and pellets from oolite iron ore in solid-phase metallization. AIP Conference Proceedings, 2456(1).

Yerbolat, M., Yesmurat, M., & Asyylbek, A. (2024). Modeling the ferrosilicomanganese smelting process using manganese-rich slag. Acta Metallurgica Slovaca, 30(1), 29–33.

Павлов, М. В., Шабанов, В. Ф., & Павлов, В. Ф. (2012). Комплексная переработка высокофосфористых марганцевых руд Новониколаевского месторождения. Химия в интересах устойчивого развития, 20(4), 443–448. // Pavlov, M. V., Shabanov, V. F., & Pavlov, V. F. (2012). Kompleksnaya pererabotka vysokofosforistykh margantsevykh rud Novonikolaevskogo mestorozhdeniya [Comprehensive processing of high-phosphorus manganese ores of the Novonikolaevsk deposit]. Khimiya v interesakh ustoychivogo razvitiya, 20(4), 443–448. (In Russ.)

Рощин, В. Е., Гамов, П. А., Рощин, А. В., & Салихов, С. П. (2023). Перспективы освоения водородных технологий в отечественной металлургии. Черная металлургия. Бюллетень НТЭИ, 79(2), 144–153. https://doi.org/10.32339/0135-5910-2023-2-144-153 // Roshchin, V. E., Gamov, P. A., Roshchin, A. V., & Salikhov, S. P. (2023). Perspektivy osvoeniya vodorodnykh tekhnologiy v otechestvennoy metallurgii [Prospects for the development of hydrogen technologies in national metallurgy]. Chernaya metallurgiya. Byulleten' NTEI, 79(2), 144–153. (In Russ.)

Tastanova, A. Y., Kuldeyev, Y. I., Temirova, S. S., Abdykirova, G. Z., & Biryukova, A. A. (2023). Processing of low-grade manganese-containing raw materials with pellet production for the manufacture of ferromanganese alloys. Engineering Journal of Satbayev University, 145, 10–18.

Government of the Republic of Kazakhstan. (2024). Concept for the development of hydrogen energy in Kazakhstan until 2030. Astana, Kazakhstan.

KazMunayGas Engineering. (2024). Assessment of underground water potential for hydrogen production needs. Atyrau, Kazakhstan.

Information about authors

Yerbol Kuatbay – Doctor of Philosophy (PhD), Karaganda Industrial University, Temirtau, Kazakhstan.
e-mail: ye.kuatbay@tttu.edu.kz
ORCID: https://orcid.org/0000-0002-8400-3537

Asylbek Nurumgaliev – Doctor of Technical Sciences, Professor, Abilkas Saginov Karaganda Technical University, Karaganda, Kazakhstan.
e-mail: anurumgaliyev@tttu.edu.kz ,
ORCID: https://orcid.org/0000-0002-8782-9975

Gulzat Bulekova – PhD doctoral student, Professor, Karaganda Industrial University, Temirtau, Kazakhstan.
e-mail: g.bulekova@tttu.edu.kz,
ORCID: https://orcid.org/0009-0008-0347-8532

Ainagul Otarbayeva – Master of Technical Sciences, K. Zhubanov Aktobe Regional University, Aktobe, Kazakhstan.
e-mail: aotarbayeva@zhubanov.edu.kz,
ORCID: https://orcid.org/0009-0005-3655-6662,

Salikhov Semyon Pavlovich – Candidate of Technical Sciences, South Ural State University (National Research University), Chelyabinsk, Russian Federation.
e-mail: salikhovsp@susu.ru ,
ORCID: https://orcid.org/0000-0002-8818-0450